



Cite this: *Environ. Sci.: Atmos.*, 2026, 6, 405

## Pollution status, source apportionment, and environmental risk assessment of trace metals in the atmospheric particulates of Islamabad, Pakistan

Rashida Nazir, Riffat Parveen and Munir H. Shah \*

This study evaluates the pollution status, source apportionment, and potential health and environmental risks of atmospheric particulates and the trace metals associated with them. Particulates were sampled on glass fibre filters in Islamabad's typical urban areas. Atomic absorption spectroscopy was employed to quantify the trace metals. Among the trace metals, Ca ( $3906 \text{ ng m}^{-3}$ ) had the highest concentration, while Ag ( $3.515 \text{ ng m}^{-3}$ ) showed the lowest concentration. The overall mean levels of the metals were in the ascending order of  $\text{Ag} < \text{Li} < \text{Cd} < \text{Co} < \text{Cu} < \text{Mn} < \text{Cr} < \text{Sr} < \text{Zn} < \text{Pb} < \text{Fe} < \text{Mg} < \text{K} < \text{Ni} < \text{Ca}$ . Particulate emission sources were identified using the multivariate PCA and CA, and it was revealed that the major pollution sources were fossil fuel combustion, local industries, road dust, and automobile emissions. The enrichment factor (EF) and the geoaccumulation index ( $I_{\text{geo}}$ ) were used to determine the contamination level. All metals exhibited EF values greater than unity ( $>1.0$ ), indicating that they predominantly originated from anthropogenic sources, except for Fe. The ecological risk assessment revealed that Ni showed the highest environmental risk ( $E_r > 320$ ) among the toxic trace metals. Similarly, the cancer risk (CR) assessment showed that the computed value for Ni was exceptionally higher than the safe limits ( $>1 \times 10^{-4}$ ), revealing an increased cancer risk for the local population. Likewise, Cr, Co, and Cd exposure were linked to significant cancer risk ( $>1 \times 10^{-6}$ ), while Pb exposure posed an insignificant cancer threat ( $<1 \times 10^{-6}$ ). The current metal concentrations in the particulates were also compared with those observed globally. Overall, the study revealed predominant anthropogenic contamination and significant health risks associated with the trace metals in atmospheric particulates.

Received 8th October 2025  
Accepted 6th January 2026

DOI: 10.1039/d5ea00131e  
rsc.li/esatmospheres

### Environmental significance

Atmospheric particulate pollution severely impacts public health and is a significant environmental problem in the major cities of Pakistan. The current study focuses on evaluating the contamination status, probable sources and associated ecological and health risks of atmospheric particulates in the urban atmosphere of Islamabad, Pakistan. Metal contents in the atmospheric particulates were found to be higher than most of the reported levels from other regions around the world, and they mostly originated from anthropogenic activities. Significant ecological and carcinogenic health risks were found to be associated with elevated toxic metal levels in atmospheric particulates, necessitating the implementation of pollution abatement strategies for improving the air quality.

## 1. Introduction

Atmospheric particulate matter (PM) is the most important environmental pollutant, which is present in varying concentrations and consists of different suspended particles with varying elemental compositions, inorganic/organic compounds, shapes, sizes, and surface properties.<sup>1</sup> The characteristics of PM are affected by geography and regional sources. Particulates are released into the atmosphere through various natural and anthropogenic sources, including soil dust, erosion, forest fires, weathering of rocks, emissions from

transportation, industrial activities, incineration, and construction activities.<sup>2-6</sup> Atmospheric particulates are one among the six criteria pollutants and are considered hazardous because of the toxic metals and harmful chemicals bound to them.<sup>7</sup>

Particulate matter pollution is a significant concern that has emerged because of rapid industrial development and socio-economic growth. It poses a severe threat to the environment, food and nutrition availability, human life, and the capability of the socioeconomic system to sustainably expand.<sup>8,9</sup> It has been estimated that particulate pollution may cause 6.50 million premature deaths annually worldwide.<sup>10</sup> The International Agency for Research in Cancer (IARC) refers to outdoor air pollution and its PM components as carcinogenic to humans.<sup>11</sup> Several studies have demonstrated that respiratory disorders,

Department of Chemistry, Quaid-i-Azam University, Islamabad 45320, Pakistan.  
E-mail: mhshahg@qau.edu.pk; munir\_qau@yahoo.com; Fax: +92-51-90642241; Tel: +92-51-90642137



cardiovascular problems, lung cancer, and even premature death are the long- and short-term detrimental health impacts of airborne particulates.<sup>12–16</sup> Toxic elements, such as lead, nickel, chromium, and cobalt, are known to stimulate the free radical mechanism by generating reactive oxygen species (ROS), which can lead to chronic health issues.<sup>5</sup> Besides damaging human health, particulate matter decreases visibility by reducing the intensity of sunlight and can cause acid rain when combined with rainwater.<sup>17–19</sup>

Trace metals associated with airborne particulate matter are distributed in the urban environment through the movement of particulates, and their accumulation in the atmosphere is lethal to living things. Several metals, including Fe, Mn, Co, Cr, Zn, and Cu, are essential to perform various physiological and biochemical functions at permissible concentrations. Exposure to excessive amounts of these metals results in poor cellular and tissue performance, ultimately leading to illness and even death.<sup>6,20</sup> Non-essential/toxic metals (Cd, Cr, Pb, and Hg) are of serious concern due to their detrimental effects even at low concentrations; for instance, Pb damages the neurological system, renal function, and peripheral nervous system. Likewise, Cr(vi) is carcinogenic to humans, causing DNA damage and cell abnormalities.<sup>5,21</sup> These are classified as poisonous substances.<sup>22</sup>

The local atmosphere of Islamabad has been significantly affected by human intrusions during the last few decades.<sup>23</sup> Recent studies reported extreme contamination and health risks due to atmospheric pollutants in the urban and rural areas of the city.<sup>24–27</sup> However, there is a lack of continuous monitoring and detailed investigations related to the trace metals' burden in atmospheric particulates. This study was designed to consider the possible impact of atmospheric particulate matter and associated toxic metals. The primary objective of this research is to investigate the levels and possible emission sources of trace metals associated with atmospheric particulate matter. In addition to assessing the extent of pollution in the area under investigation, this study aims to evaluate the ecological and human health risks posed by these metals. Overall, this study's findings will contribute towards assessing the environmental and health impacts of particulate pollution, and developing effective strategies to mitigate the risks associated with trace metals in particulate matter.

## 2. Materials & methods

### 2.1 Study area

The sampling was conducted in Islamabad (33° 49'N and 72° 24'E), the federal capital of Pakistan, which is situated at around 500 m above sea level and has a land area of 906.5 km<sup>2</sup> (Fig. 1). It is 14 km northeast of its twin city Rawalpindi, which shares close social and business relationships with the capital city. The federal city is flanked by the Margalla Hills to the north, and the plains of Punjab and water bodies on the other sides. Islamabad is home to 2 million people, as per the 2017 census.<sup>25</sup> The urban area of Islamabad is segregated into eight distinct areas, including parks, green zones, residential, official, commercial, and business. The main industries in the industrial zones of the

city (sectors of I-9, I-10, and Kahuta Triangle) include steel mills, pottery, flour mills, paint, dyes, metallurgy, medicinal/chemical plants, earthenware, granite, and oil and ghee plants. Industrial emissions, construction work and vehicle exhausts are the main sources of air pollution in the city.

Islamabad has a subtropical climate with a hot summer in June, monsoons in July and August, and cold winter in December and January. Significant meteorological fluctuations have been observed in Islamabad over the past few years. In June, the weather is extremely hot, with temperatures soaring as high as 50 °C, while the temperature may plummet to as low as –2 °C during cold winter days. The wind predominantly blows from the northeast, with average daytime velocities reaching up to 0.86 m s<sup>–1</sup> and dropping to approximately 0.50 m s<sup>–1</sup> at night.<sup>24,25</sup> Islamabad's geology is characterized by folded sedimentary rocks (Jurassic to Paleocene) forming the Margalla Hills. This tectonically active area experiences seismic hazards, with underlying soft sediments varying in thickness. The region primarily consists of marine and continental sediments, including limestones, shales, and sandstones. The area is structurally complex due to tectonic forces from the India-Eurasia collision, leading to significant folding and active fault lines.<sup>28</sup>

### 2.2 Sampling

The sampling was performed following the USEPA standard method<sup>29</sup> during the summer (June to September) and autumn (October to November) seasons in a typical urban area of the Quaid-i-Azam University campus. A sequential air sampler (DPM5, AMS Analytica, Italy) was used to collect the total suspended particulate (TSP) samples on glass fibre filters. The sampler was installed on the roof-top approximately 15 m above the ground level and well cleared from other nearby tall buildings. Approximately 2 to 3 samples were collected per week on alternate days. The sampling was performed in 12–24 h intervals (excluding public holidays), starting at 09:00 h and a total of 53 TSP samples were collected. The filters were equilibrated in a moisture-controlled desiccator for 24 h before and after sampling. The weight of the filter papers was determined before and after sample collection and stored in plastic bags. The mass of the particulates was calculated gravimetrically.<sup>30</sup> Blanks were also included in each batch and treated the same as the samples.

### 2.3 Sample preparation

Sample solutions for trace metal analysis were prepared using the standard methodology approved by USEPA.<sup>31</sup> The hot acid extraction technique was used to extract the metals. The filter papers containing the particulates were folded in half lengthwise with the particulate material facing inward and cut into 1" × 8" strips. The filter paper strips were placed in the lower portion of the marked 100 mL flask to ensure the acid volume covered the entire filter paper. Then, 50 mL of the extraction solution (5.6% HNO<sub>3</sub> and 16.8% HCl, v/v) was added to the vessel and placed on a hot plate in a fume hood. The liquid was carefully refluxed for 60 minutes, while covered by a watch



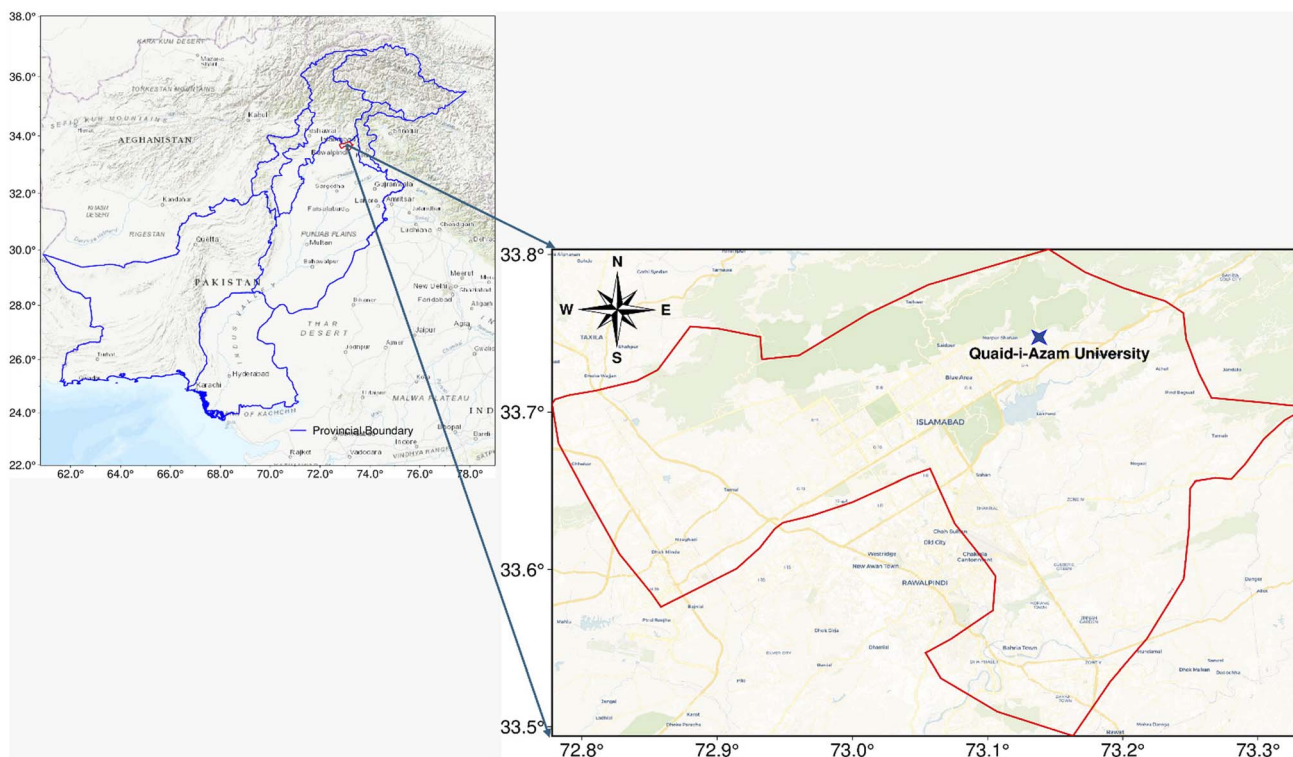


Fig. 1 Location map of the study area (X) in Islamabad, Pakistan.

glass. The flask was then removed from the hot plate and allowed to cool. The digestate was filtered using Whatman filter paper, and each solution was transferred to a 50 mL volumetric flask and diluted with a 0.1 N nitric acid solution. The same method was used to prepare the blanks containing only filter paper. All reagents used were of analytical grade (certified purity > 99.9%) and procured from Merck (Darmstadt, Germany) or BDH (UK). Doubly distilled water was used throughout the present work.

#### 2.4 Metals' quantification

Quantitative analysis of the metals (Fe, Ca, Mg, Zn, Mn, Cu, Co, Sr, K, Ag, Li, Cd, Cr, Ni, and Pb) in all samples was performed by atomic absorption spectrometry (Shimadzu AA-670, Japan) using the standard procedure.<sup>32</sup> Quantification of the metals in the samples was performed under optimum analytical conditions, as shown in Table S1 (SI), following the calibration line method, which showed an excellent correlation coefficient (>0.990). Each metal's standard stock solution (1000 mg L<sup>-1</sup>) was used to prepare fresh working standards. The standard reference material (NIST SRM-2711) was employed and analysed to ensure the accuracy of the measured metal data, as shown in Table S2 (SI), which revealed excellent recovery. An inter-laboratory data comparison was also performed, demonstrating the best agreement with each other (less than a 2% difference). The blank input for all metals was assessed and noted to be less than 5% of the measured metal levels. All glassware was thoroughly cleaned after an overnight soak in a 5% HNO<sub>3</sub> solution. After that, it was rinsed with doubly distilled water and dried in

an oven at 70 °C. During the investigation, analytical-grade acid, glassware and reagents were employed.

#### 2.5 Statistical analysis

The analysed data were employed for a descriptive statistical analysis, which included calculating the maximum, minimum, median, mean, standard deviation, kurtosis, and skewness. The analysis demonstrated how the different data set variables were distributed, varied, and dispersed. The mutual relationship among the variables was investigated by computing the correlation coefficient. Moreover, major pollution sources and activities were assessed using multivariate statistical methods, including cluster analysis (CA) and principal component analysis (PCA).

#### 2.6 Pollution assessment

The pollution level was evaluated by determining the enrichment factor (EF) and geoaccumulation index ( $I_{geo}$ ). The enrichment factor was employed to determine whether the metal sources were natural or anthropogenic. It is a suitable method for identifying emission sources and was estimated by applying the following relationship:

$$EF = \frac{[X/M_{ref}]_{sample}}{[X/M_{ref}]_{crust}} \quad (1)$$

where  $X$  is the target metal concentration,  $M_{ref}$  is the reference metal concentration in the analysed samples and background soil, and EF is the enrichment factor. Although several metals



could serve as the reference, the choice of Fe was made based on its abundance in both the samples and the background soil. The metal levels in the upper continental crust were taken as the background level in the present study.<sup>33</sup> In general,  $EF < 10$  indicates that the dominant metal source is the earth's crust, while  $EF > 10$  shows that human activities have contributed to the enrichment of the samples. An  $EF$  of 10–100 indicates that the metals are moderately enriched, while an  $EF > 100$  denotes irregular enrichment of the metals in the particulates.<sup>34,35</sup>

The geoaccumulation index ( $I_{geo}$ ) is a geochemical parameter that determines the particle pollution levels and contaminants. It was calculated using the following relationship:

$$I_{geo} = \log_2 \left( \frac{C_n}{1.5B_n} \right) \quad (2)$$

where " $C_n$ " is the detected metal levels of particulate samples, and " $B_n$ " is the geochemical background value of the metals in the soil.<sup>33</sup> The factor of 1.5 is used to identify minimal anthropogenic influences and reduce the possible changes in pre-industrial values due to lithogenic effects. The  $I_{geo}$  can be interpreted as follows:  $I_{geo}$  values less than 0 suggest that there is no contamination;  $0 < I_{geo} \leq 1$  shows uncontaminated to moderately contaminated;  $1 < I_{geo} \leq 2$  exhibits moderate contamination;  $2 < I_{geo} \leq 3$  exhibits moderate-to-heavy contamination;  $3 < I_{geo} \leq 4$  displays heavy contamination;  $4 < I_{geo} \leq 5$  shows severe contamination, and  $I_{geo} \geq 5$  indicates the most serious contamination.

## 2.7 Ecological risk assessment

The natural ecological equilibrium in the atmosphere can be disturbed by high metal concentrations, which are hazardous to living organisms. The environmental risk index (RI) has been widely used to assess the level of trace metals in particulate matter. The relationships shown below are used to calculate the RI:

$$RI = \sum_{i=1}^m E_r^i \quad (3)$$

$$E_r^i = T_r^i \frac{C_{sample}^i}{C_{crust}^i} \quad (4)$$

where  $E_r$  is the metal's potential ecological risk coefficient and  $T_r$  is the metal's toxic reaction factor.<sup>36</sup> It is related to the distribution capacity and relative abundance of the metal pollutant in various forms, including metamorphic rocks, soil, freshwater, continental plants, animals, *etc.*

## 2.8 Health risk assessment

Metals reach the body of an individual *via* three major paths: oral ingestion, direct inhalation, and adsorption/skin contact. However, direct inhalation is regarded as the main exposure route. Therefore, in the present investigation, exposure through inhalation was evaluated and calculated as per USEPA methodology.<sup>37</sup>

$$EC_{inh} = C \times \frac{ET \times EF \times ED}{AT_n} \quad (5)$$

where  $C$  is the exposure concentration,  $ET$  is the exposure time,  $ED$  is the exposure duration,  $EF$  is the exposure frequency, and  $AT_n$  is the average lifetime.

Non-carcinogenic and carcinogenic effects were evaluated for risk characterization. The non-carcinogenic risks were estimated by computing the hazard quotient (HQ) using USEPA methodology.<sup>14,37</sup>

$$HQ_{inh} = \frac{EC_{inh}}{RfC_i \times 1000} \quad (6)$$

Here,  $RfC_i$  is the inhalation reference concentration ( $\mu\text{g m}^{-3}$ ). Usually, HQ values greater than unity are considered hazardous for exposed populations. The overall non-carcinogenic risks were assessed by determining the hazard index (HI), which is the sum of the HQs of all metals. Here again,  $HI \leq 1$  suggests that there is no potential health risk, and  $HI \geq 1$  implies that there is a non-carcinogenic health risk.<sup>21</sup>

Carcinogenic risk (CR) was estimated by calculating the cumulative probability of a person developing cancer throughout the lifetime due to toxic metal exposure by inhalation. The carcinogenic risk of toxic metals was determined using the following relationship:<sup>37</sup>

$$CR_{inh} = EC_{inh} \times IUR \quad (7)$$

Here,  $CR_{inh}$  is a cancer risk a person faces because of inhaling a specific carcinogenic metal. The IUR refers to the inhalation unit risk. The USEPA suggests that  $CR \leq 1.0 \times 10^{-6}$  be deemed insignificant, while  $CR \geq 1.0 \times 10^{-4}$  is considered to have detrimental impacts on humans.

## 3. Results & discussion

### 3.1 Distribution of TSP and trace metals

The basic distribution parameters that were used to evaluate the levels of TSP and trace metals in this investigation are shown in Table 1. A considerable variation in the concentration of TSP was found, ranging from a minimum of  $45.00 \mu\text{g m}^{-3}$  to a maximum of  $480.3 \mu\text{g m}^{-3}$ , with an average level of  $157.3 \mu\text{g m}^{-3}$ . The significantly higher SD and SE values supported higher TSP variability and random distribution. At the same time, skewness and kurtosis data suggested that the dispersion of airborne particles was moderately skewed. The mean level of  $157.3 \mu\text{g m}^{-3}$  was higher than the WHO ( $150 \mu\text{g m}^{-3}$ ) standards.<sup>38</sup> The mean level of TSP showed a notable decrease in the concentration ( $157.3 \mu\text{g m}^{-3}$ ) of particulate matter when compared with previously reported data. For instance, Shahid *et al.*<sup>26</sup> reported that the mean level of TSP was  $343 \mu\text{g m}^{-3}$  in the atmosphere of Islamabad, which was remarkably higher than the present level. Overall, particulate matter pollution has decreased.

The statistical distribution parameters for the metals are shown in Table 1. Ca exhibited the highest concentration ( $3906 \text{ ng m}^{-3}$ ) among the metals in the total suspended particulate matter, followed by Ni ( $3657 \text{ ng m}^{-3}$ ), K ( $3091 \text{ ng m}^{-3}$ ), Mg ( $1198$



**Table 1** Statistical distribution parameters for TSP ( $\mu\text{g m}^{-3}$ ) and concentrations of trace metals ( $\text{ng m}^{-3}$ ) in atmospheric particulate matter

|     | Min   | Max   | Mean  | Median | SD    | SE    | Kurtosis | Skewness |
|-----|-------|-------|-------|--------|-------|-------|----------|----------|
| TSP | 45.00 | 480.3 | 157.3 | 126.6  | 85.79 | 11.78 | 2.641    | 1.374    |
| Cr  | 4.447 | 171.2 | 44.41 | 20.01  | 50.05 | 7.632 | 0.352    | 1.306    |
| Ni  | 200.0 | 6800  | 3657  | 2790   | 2153  | 399.8 | -1.592   | 0.123    |
| Cd  | 1.095 | 10.69 | 4.296 | 3.597  | 2.706 | 0.403 | -0.364   | 0.809    |
| Pb  | 11.46 | 362.3 | 106.6 | 65.82  | 91.21 | 14.61 | 0.867    | 1.292    |
| Cu  | 1.368 | 72.80 | 18.62 | 14.34  | 15.94 | 2.431 | 2.713    | 1.527    |
| Co  | 2.976 | 40.04 | 14.91 | 11.90  | 11.03 | 1.920 | -0.160   | 0.950    |
| Ag  | 0.271 | 8.894 | 3.515 | 3.247  | 2.245 | 0.351 | 0.002    | 0.759    |
| Zn  | 13.68 | 278.7 | 75.91 | 57.84  | 58.64 | 9.912 | 2.828    | 1.505    |
| Mn  | 2.866 | 110.7 | 32.51 | 23.83  | 26.20 | 3.633 | 0.632    | 1.161    |
| Li  | 0.342 | 9.921 | 4.203 | 3.558  | 2.511 | 0.383 | -0.316   | 0.653    |
| Mg  | 158.2 | 3922  | 1198  | 868.3  | 974.4 | 164.7 | 0.402    | 1.029    |
| Ca  | 376.3 | 9248  | 3906  | 3250   | 2478  | 369.5 | -0.532   | 0.691    |
| Sr  | 12.14 | 168.2 | 55.78 | 44.98  | 37.36 | 5.449 | 1.330    | 1.273    |
| K   | 701.3 | 6511  | 3091  | 2990   | 1729  | 284.3 | -0.890   | 0.493    |
| Fe  | 123.1 | 5359  | 1010  | 595.0  | 1100  | 169.7 | 6.086    | 2.298    |

$\text{ng m}^{-3}$ ), Fe ( $1010 \text{ ng m}^{-3}$ ), and Pb ( $106.6 \text{ ng m}^{-3}$ ). In contrast, Cd ( $4.296 \text{ ng m}^{-3}$ ), Li ( $4.203 \text{ ng m}^{-3}$ ), and Ag ( $3.515 \text{ ng m}^{-3}$ ) were found to be the lowest mean contributors. Moreover, toxic metals, including Cd, Pb, and Cr, were found in the air within safe limits, except for Ni, which was found to be above the recommended values set by the World Health Organisation (WHO). The levels recommended by WHO are  $5 \text{ ng m}^{-3}$ ,  $500 \text{ ng m}^{-3}$ , and  $25 \text{ ng m}^{-3}$  for Cd, Pb, and Ni, respectively.<sup>39</sup> Elevated levels of Ni in the local atmosphere were mainly associated with fossil fuel combustion and industrial emissions in the city. The overall mean metal levels were observed to increase in the following order: Ag < Li < Cd < Co < Cu < Mn < Cr < Sr < Zn < Pb < Fe Mg K < Ni < Ca. These findings are consistent with the results of Liu *et al.*,<sup>15</sup> providing further support for the present investigation. Moreover, the study investigated the dispersion and distribution of metals in the urban environment. The results

indicated that most of the metals exhibited large dispersion and random distribution, as evidenced by their large range, higher standard deviations, and diverse mean and median values, as depicted in Table 1 and Fig. S1 (SI). The highest dispersion around the average values was observed in the cases of Ca, Ni, K, Mg, Fe, and Pb, while Ag, Li, Cd, and Co showed relatively small dispersion. The standard deviation and standard error values revealed that most metals had a random distribution pattern, supported by the symmetry parameters skewness and kurtosis, which indicated that anthropogenic emissions impact the urban environment.

Compared to previous data reported by Ahmed *et al.*,<sup>23</sup> the current average concentration of some metals showed different trends. For instance, a few metal levels, including Pb, Cd, Zn, and Cr, increased while the rest of them decreased, indicating the diversity of regional sources. Soil dirt, cement production, steel dust, and power plant dust are the primary sources of Ca, Fe, K, and Mg,<sup>40</sup> whereas Ni and Cr are produced by burning coal and industrial processes. Cu is released into the atmosphere due to tyre and brake abrasion, whereas galvanized gasoline tanks and traffic emissions contribute Zn to the urban atmosphere.<sup>41</sup> Overall, the findings of this study provide valuable insights into the dispersion and distribution of metals in the urban atmosphere. The results suggested that anthropogenic emissions had a significant impact on the environment, and the diversity of regional sources contributed to the variability in metal concentrations.

### 3.2 Correlation study

The correlation coefficient data are shown in Table 2, with the bold  $r$  value significant at  $p < 0.05$ . This value demonstrates a strong and mutual correlation between TSP and metals as well as in the concentrations of the metal pairs. TSP was notably correlated with Mn and Mg metals. Meanwhile, among the trace metals, Fe–Mn ( $r = 0.788$ ), Zn–Cr ( $r = 0.709$ ), Cu–Pb ( $r = 0.707$ ), Mn–Cu ( $r = 0.686$ ), Mg–Mn ( $r = 0.648$ ), and Sr–Mn ( $r = 0.638$ )

**Table 2** Correlation coefficient<sup>a</sup> matrix for TSP and selected metal levels in the atmospheric particulate matter

|     | TSP          | Cr            | Ni            | Cd            | Pb           | Cu           | Co            | Ag           | Zn           | Mn           | Li           | Mg           | Ca    | Sr           | K      | Fe    |
|-----|--------------|---------------|---------------|---------------|--------------|--------------|---------------|--------------|--------------|--------------|--------------|--------------|-------|--------------|--------|-------|
| TSP | 1.000        |               |               |               |              |              |               |              |              |              |              |              |       |              |        |       |
| Cr  | -0.161       | 1.000         |               |               |              |              |               |              |              |              |              |              |       |              |        |       |
| Ni  | 0.172        | <b>0.382</b>  | 1.000         |               |              |              |               |              |              |              |              |              |       |              |        |       |
| Cd  | -0.222       | -0.005        | -0.195        | 1.000         |              |              |               |              |              |              |              |              |       |              |        |       |
| Pb  | 0.169        | -0.084        | 0.241         | <b>-0.390</b> | 1.000        |              |               |              |              |              |              |              |       |              |        |       |
| Cu  | 0.099        | 0.024         | 0.080         | -0.103        | <b>0.707</b> | 1.000        |               |              |              |              |              |              |       |              |        |       |
| Co  | -0.173       | 0.297         | -0.120        | 0.234         | -0.103       | -0.157       | 1.000         |              |              |              |              |              |       |              |        |       |
| Ag  | -0.215       | 0.179         | -0.131        | 0.153         | 0.108        | -0.002       | <b>0.333</b>  | 1.000        |              |              |              |              |       |              |        |       |
| Zn  | 0.057        | <b>0.709</b>  | -0.013        | -0.077        | 0.075        | 0.063        | <b>0.473</b>  | 0.125        | 1.000        |              |              |              |       |              |        |       |
| Mn  | <b>0.335</b> | -0.046        | -0.074        | <b>-0.334</b> | <b>0.520</b> | <b>0.686</b> | -0.224        | 0.052        | -0.168       | 1.000        |              |              |       |              |        |       |
| Li  | -0.071       | <b>0.327</b>  | -0.119        | -0.273        | 0.269        | <b>0.325</b> | 0.203         | <b>0.495</b> | <b>0.565</b> | <b>0.348</b> | 1.000        |              |       |              |        |       |
| Mg  | <b>0.387</b> | <b>-0.417</b> | <b>-0.312</b> | <b>-0.419</b> | <b>0.589</b> | <b>0.461</b> | <b>-0.471</b> | -0.273       | -0.204       | <b>0.648</b> | 0.208        | 1.000        |       |              |        |       |
| Ca  | 0.032        | 0.149         | 0.086         | 0.168         | 0.203        | <b>0.584</b> | -0.161        | -0.026       | 0.063        | <b>0.370</b> | 0.182        | 0.153        | 1.000 |              |        |       |
| Sr  | 0.042        | 0.105         | -0.045        | <b>-0.363</b> | <b>0.303</b> | <b>0.397</b> | <b>-0.435</b> | 0.048        | -0.118       | <b>0.638</b> | <b>0.385</b> | <b>0.421</b> | 0.278 | 1.000        |        |       |
| K   | -0.014       | -0.005        | -0.119        | 0.108         | 0.294        | 0.296        | <b>0.452</b>  | 0.236        | 0.171        | -0.001       | -0.052       | -0.127       | 0.167 | -0.228       | 1.000  |       |
| Fe  | 0.130        | -0.195        | -0.155        | <b>-0.430</b> | <b>0.393</b> | <b>0.365</b> | <b>-0.318</b> | -0.020       | -0.206       | <b>0.788</b> | 0.196        | <b>0.576</b> | 0.073 | <b>0.590</b> | -0.067 | 1.000 |

<sup>a</sup>  $r$ -Values shown in bold are significant at  $p < 0.05$ .

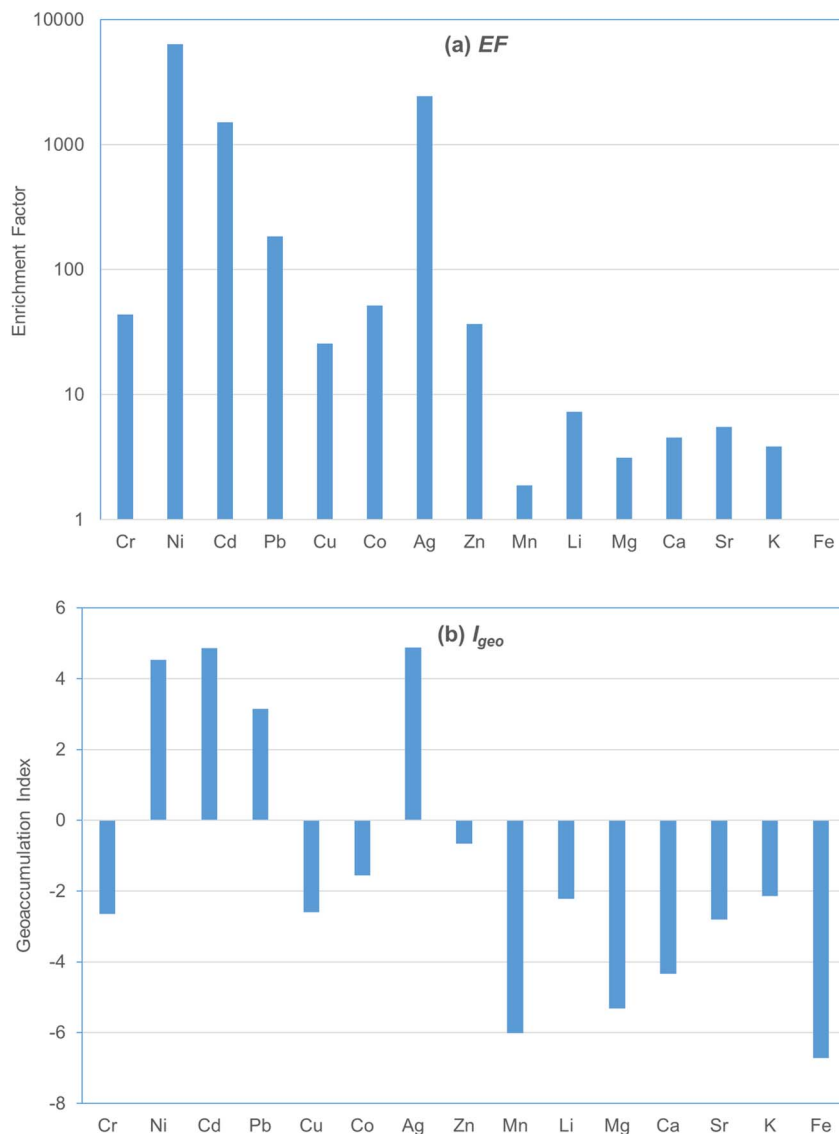


Fig. 2 Comparison of the average (a) enrichment factors and (b) geoaccumulation indices of selected metals in atmospheric particulates.

had the strongest correlation. Similarly, a statistically substantial correlation was observed among Fe–Sr ( $r = 0.590$ ), Mg–Pb ( $r = 0.589$ ), Li–Zn ( $r = 0.565$ ), Pb–Mn ( $r = 0.520$ ), Ca–Cu ( $r = 0.584$ ), and Fe–Mg ( $r = 0.576$ ). Based on the correlation coefficient data, the trace metals could be classified into two groups: the first group comprises Zn, Mn, Cr, Cu, Pb, Mg, and Sr, while the other is made up of Fe, Sr, Li, Mg, and Ca. The correlation pattern suggests that Ca, Fe, Mg, and Li were emitted into the atmosphere through natural sources, mainly wind-blown soil and the earth's crust. Zn, Mn, Cr, Pb, and Sr were released by some familiar sources, probably human activities. The findings of this research are well supported by the results of Baidourela *et al.*<sup>9</sup> In airborne particulate matter, some metal pairs showed a negative correlation, including Fe–Cd ( $r = 0.430$ ), Mg–Cr ( $r = 0.417$ ), and Co–Sr ( $r = 0.435$ ), revealing their contrasting fluctuations in the atmospheric particulate matter, which indicate that there was no apparent common source of airborne

particles. In airborne particulate matter, some metal pairs showed a negative correlation, including Fe–Cd ( $r = 0.430$ ), Mg–Cr ( $r = 0.417$ ), and Co–Sr ( $r = 0.435$ ), revealing their contrasting fluctuations in atmospheric particulate matter. A negative correlation also indicates that there was no apparent common source of airborne particles.

### 3.3 Pollution assessment

The enrichment factors (EF) and geoaccumulation indices ( $I_{geo}$ ) were used to assess how anthropogenic emissions influenced the level of trace metals in airborne particles. The estimated EF helps to identify the anthropogenic sources of the metals in TSP. Normally, EF values of less than 10 indicate that metals are released primarily from crustal sources, and values greater than 10 may suggest that sources are anthropogenic. Fig. 2a displays the EF values of each trace metal. From the enrichment factor levels, the metals were clustered as extremely enriched (EF



Table 3 Principal component analysis of TSP and selected metal levels in the atmospheric particulate matter

|                         | PC 1   | PC 2   | PC 3   | PC 4   | PC 5   | PC 6   |
|-------------------------|--------|--------|--------|--------|--------|--------|
| Eigen value             | 4.010  | 2.334  | 1.568  | 1.438  | 1.300  | 1.050  |
| Total variance (%)      | 25.06  | 14.59  | 9.798  | 8.987  | 8.127  | 6.561  |
| Cumulative variance (%) | 25.06  | 39.65  | 49.45  | 58.44  | 66.56  | 73.12  |
| TSP                     | -0.237 | -0.010 | -0.112 | 0.723  | 0.046  | 0.060  |
| Cr                      | -0.157 | 0.770  | -0.147 | 0.131  | 0.130  | -0.309 |
| Ni                      | 0.041  | -0.028 | 0.032  | 0.073  | -0.039 | 0.953  |
| Cd                      | 0.593  | 0.176  | -0.069 | -0.263 | -0.393 | -0.242 |
| Pb                      | 0.678  | 0.022  | 0.387  | -0.098 | 0.163  | -0.278 |
| Cu                      | 0.444  | 0.061  | 0.241  | -0.075 | 0.688  | -0.058 |
| Co                      | -0.273 | 0.266  | 0.583  | 0.251  | -0.212 | 0.066  |
| Ag                      | 0.142  | 0.125  | 0.325  | 0.723  | -0.084 | 0.034  |
| Zn                      | -0.115 | 0.876  | 0.190  | -0.131 | 0.009  | 0.068  |
| Mn                      | 0.822  | 0.022  | -0.045 | -0.053 | 0.264  | 0.068  |
| Li                      | 0.416  | 0.680  | 0.042  | 0.266  | 0.039  | 0.140  |
| Mg                      | 0.700  | -0.136 | -0.046 | -0.404 | 0.136  | 0.277  |
| Ca                      | 0.091  | 0.098  | -0.028 | -0.010 | 0.885  | -0.032 |
| Sr                      | 0.677  | 0.086  | -0.436 | 0.195  | 0.230  | -0.018 |
| K                       | -0.029 | -0.033 | 0.790  | 0.031  | 0.225  | 0.015  |
| Fe                      | 0.800  | -0.147 | -0.148 | 0.026  | 0.005  | 0.086  |

greater than 100), including Ni, Ag, and Cd; moderately enriched (EF values between 10 and 100), including Pb, Co, Cr, Zn, and Cu; and less enriched (EF less than 10): Li, Mg, Sr, Ca, Mn, and K. The highest EF values were shown by Ni and Ag, followed by those of Cd and Pb. The highest EF values demonstrated that the anthropogenic emissions significantly influenced the metals in the airborne particulates. Metals, including Pb, Cd, and Zn, are emitted by automobile exhaust, while local metal industries release Fe, Cu, and Co into the surrounding environment.<sup>42</sup> In contrast, the less-enriched metals with EF values of less than 1 (Li, Ca, Mn, K, and Sr) primarily originated from the earth's crust and the resuspension of soil particles.<sup>43</sup> These results are comparable with those reported by Panda *et al.*<sup>20</sup> Overall, all metals exhibited EF values greater than unity, indicating that they are believed to originate predominantly from anthropogenic sources except for Fe.

The geoaccumulation index ( $I_{geo}$ ) is used to describe the extent of environmental pollution. Fig. 2b displays the mean  $I_{geo}$  of the selected elements. Some of the metals, including Ag, Cd, and Ni, had values of  $I_{geo} \geq 4$  and showed the highest contamination levels. In contrast, Pb had moderate to heavy contamination in the atmospheric particulate matter with  $I_{geo} \geq 2$ . The remaining metals had  $I_{geo} \leq 0$ , demonstrating their uncontaminated presence in the airborne particles. Similar results for hazardous metals are reported in the literature.<sup>20,34,43</sup> The results of the pollution assessment indicate that the presence of Ag, Cd, Ni, and Pb has had a significant impact on the surrounding environment, leading to severe atmospheric pollution in the local area.

### 3.4 Multivariate source apportionment

The source identification/apportionment of trace metals in airborne particles is one of the most significant parts of this study. It was accomplished using principal component analysis

(PCA) and cluster analysis (CA). Table 3 provides the principal component (PC) loadings of TSP and selected metals, whereas Fig. S2 (SI) shows the corresponding CA. A total of six PCs with Eigen values > 1 were retrieved by normalised rotation on datasets for particulates, accounting for about 73.12% of the total variance (Table 3). PC 1 had the highest loadings for metals, including Mn, Fe, and Mg, accounting for 25.06% of the total variance. The CA also observed a cluster comprising the same metals. These metals were known to be associated with the earth's crust and wind-blown soil in the atmosphere.<sup>15</sup> Therefore, this cluster is mostly controlled by local geological settings of the study area. The highest loading in favour of Zn, Cr, and Li was observed in PC 2 with a total variance of 14.59%, indicating that these were derived from familiar sources, especially industrial emissions from metallurgical and electrical components located in industrial areas of the city.<sup>43</sup> PC 3 showed the highest loadings for K and Co. These metals were derived from burning and incineration.<sup>44</sup> The highest TSP and

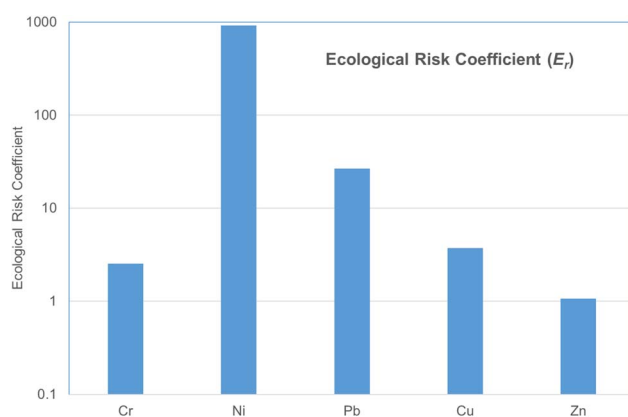


Fig. 3 Average values of the ecological risk coefficients ( $E_r$ ) of trace metals in atmospheric particulates.



Ag loadings were found in PC 4, with total variances of 9.79% and 8.98%, respectively. PC 5 revealed the highest loadings for Ca, mainly emitted from crustal material and hence geogenic in origin. The last PC showed the highest loading for Ni, which is released into the atmosphere from transportation, oil, and coal combustion.<sup>9</sup> The application of multivariate PCA and CA revealed that anthropogenic emissions played a significant role in the occurrence of trace metals in airborne particulates. This finding is further supported by the enrichment factors (EF) and geoaccumulation index ( $I_{geo}$ ). These results suggest that anthropogenic activities are a major contributor to the presence of trace metals in airborne particulates.

### 3.5 Ecological risks

The ecological risks caused by toxic metals in TSP were assessed using an ecological risk index (RI) and an ecological risk coefficient ( $E_r$ ). Risk index (RI) is a total risk index that is typically classified as follows: RI < 150 shows low environmental risk, RI < 300 shows moderate ecological risk, RI < 600 specifies significant environmental risk, and RI  $\geq$  600 means extremely high ecological risk.<sup>34,36,45</sup> The ecological risk coefficients for every single metal can be separated into five groups based on their  $E_r$  values:<sup>36</sup> low risk ( $E_r < 40$ ), moderate risk ( $E_r < 80$ ), significant risk ( $E_r < 160$ ), highest risk ( $E_r > 160$ ), and the extreme risk ( $E_r > 320$ ). Fig. 3 displays the ecological risk coefficient of selected trace metals. It was revealed that metals such as Zn, Cr, and Cu showed a low ecological risk, whereas Pb had a moderate risk ( $E_r < 80$ ) and Ni exhibited a remarkably high risk ( $E_r > 320$ ). Overall, metals in TSP pose an ecological risk in the following order: Ni > Pb > Cu > Cr > Zn. These elements are very toxic pollutants in the atmosphere. It is essential to lower their emission levels, particularly for Ni. The cumulative risk index (RI) for metals was very high, with RI > 600, indicating an extremely high ecological risk. It is concluded that the current metal concentrations in the local atmosphere caused a very high ecological risk during the sampling period, and Ni was the main contributor to that risk. Hence, controlling or decreasing these harmful elements' emission sources into the local atmosphere is necessary.

### 3.6 Health risks

The most essential part of this study was the evaluation of the potential health risks caused by toxic metals in airborne particles. Inhalation represents the most prevalent route through which individuals are directly exposed to particulate metals in the air. Fig. 4a displays the average exposure levels of toxic elements through inhalation of airborne particles. The exposure concentration of toxic metals, including Ca, K, Mg, and Fe, was comparatively high. However, these metals are not usually considered detrimental because they are essential to life and do not have any toxic impacts on health. In contrast, the metals Pb, Zn, Sr, and Mn all had slightly high exposure levels. However, continuous and regular exposure to these metals in elevated concentrations harms human health. The non-carcinogenic health risks caused by toxic metals were assessed using the hazard quotient (HQ) and hazard index (HI). Fig. 4b shows the

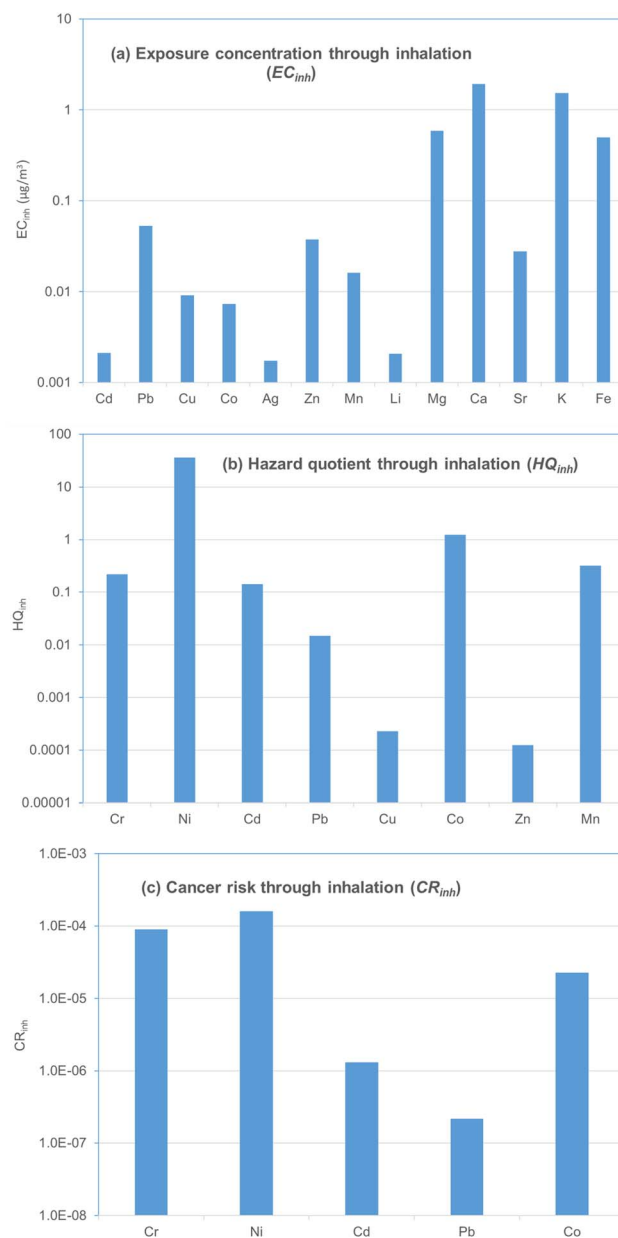


Fig. 4 Average levels of (a) exposure concentrations ( $\mu\text{g m}^{-3}$ ), (b) hazard quotients and (c) carcinogenic risks of trace metals through the inhalation of TSP.

average HQ for the hazardous elements. An HQ value of less than one (1.0) is considered safe. The computed HQ values for Ni and Co metals exceeded the safe limit ( $HQ > 1$ ), indicating possible non-cancer risks to humans. The rest of the metals (Mn, Cr, Cd, Pb, Cu, and Zn) had HQ values within the safe limit ( $HQ < 1$ ); therefore, no significant non-carcinogenic risks were linked with their exposure *via* inhalation of airborne particles. The results of this study agreed with those of Ulutas.<sup>35</sup> Moreover, the HI value was above the safe limit ( $HI > 1$ ), revealing the non-carcinogenic risks caused by toxic metals in TSP.

The assessment of the cancer risks (CR) caused by inhaling toxic metals is illustrated in Fig. 4c. Cancer risk (CR) is commonly interpreted as follows: when the computed CR value



Table 4 Comparison of the present mean levels of TSP ( $\mu\text{g m}^{-3}$ ) and trace metals ( $\text{ng m}^{-3}$ ) with the reported levels around the world

| Site                                | TSP    | Cr     | Ni   | Cd    | Pb     | Cu     | Co    | Ag    | Zn     | Mn     | Li    | Mg    | Ca    | Sr    | K     | Fe     |
|-------------------------------------|--------|--------|------|-------|--------|--------|-------|-------|--------|--------|-------|-------|-------|-------|-------|--------|
| Islamabad (Pakistan) <sup>a</sup>   | 157.3  | 44.41  | 3657 | 4.296 | 106.6  | 18.62  | 14.91 | 3.515 | 75.91  | 32.51  | 4.203 | 1198  | 3906  | 55.78 | 3091  | 1010   |
| Islamabad (Pakistan) <sup>26</sup>  | 343    |        |      |       |        |        |       |       |        |        |       |       |       |       |       |        |
| Lahore (Pakistan) <sup>47</sup>     | 23460  | 860    | 6790 |       | 3880   | 2160   |       |       | 10630  | 1510   |       | 2970  | 4160  |       | 1510  | 16090  |
| Dhaka (Bangladesh) <sup>56</sup>    |        |        | 110  |       | 633    | 110    |       |       | 1640   | 460    |       | 78000 | 17700 | 170   | 54000 | 860    |
| Delhi (India) <sup>48</sup>         | 739    | 190    | 70   | 30    | 250    | 70     | 20    | 30    | 900    | 3240   | 10    |       |       |       |       | 11020  |
| Kathmandu (Nepal) <sup>49</sup>     | 264    |        |      |       |        |        |       |       |        |        |       |       |       |       |       |        |
| Beijing (China) <sup>21</sup>       | 152    | 22.2   | 12.2 | 4.7   | 193    | 115    | 3.5   |       | 476    | 156.81 |       | 3410  | 14700 |       | 2770  | 6170   |
| Huainan (China) <sup>43</sup>       | 389.84 |        |      |       |        |        |       |       | 249.34 |        |       |       |       |       |       |        |
| Qingdao (China) <sup>15</sup>       |        | 46.5   | 32.5 | 13.8  | 291.7  | 164.9  |       |       | 23.99  | 355.1  | 13.9  | 3736  | 16263 | 97.3  | 5020  | 9192   |
| Tehran (Iran) <sup>57</sup>         | 27.48  |        |      |       | 23.59  |        |       |       | 4252   |        | 0.010 | 10.70 |       | 3.53  |       | 15.70  |
| Zabol (Iran) <sup>14</sup>          | 1624   |        |      | 20    | 780    | 130    | 20    |       |        |        |       | 2400  | 9100  |       | 1600  | 3100   |
| Jeddah (Saudi Arabia) <sup>53</sup> | 125    |        |      |       |        |        |       |       |        |        |       |       |       |       |       |        |
| Kampar (Malaysia) <sup>58</sup>     | 90.99  |        |      |       |        |        |       |       |        |        |       |       |       |       |       |        |
| Maros (Indonesia) <sup>52</sup>     | 156.86 | 81.170 |      |       | 746780 | 78950  |       |       |        |        |       |       |       |       |       |        |
| Seoul (South Korea) <sup>10</sup>   | 83.87  |        | 5.4  | 1.22  | 34.0   |        | 0.75  |       | 137    | 41.1   |       | 483   | 1750  |       | 505   | 1760   |
| Pohang (South Korea) <sup>50</sup>  | 106.9  | 0.3    | 14.3 | 1.2   | 63.6   |        | 1.1   |       | 204.5  | 253.3  |       |       |       |       |       | 3.4    |
| Hat Yai (Thailand) <sup>51</sup>    | 58.3   | 0.16   | 0.32 |       | 1.27   | 2.11   |       |       | 10.87  | 3.52   |       | 111.4 |       |       | 313.3 | 74.6   |
| Yenagoa (Nigeria) <sup>59</sup>     |        | 0.8    | 12.6 | 1.7   | 5.3    | 4.3    | 1.6   |       | 58     | 4.4    |       |       | 2167  |       |       | 653.9  |
| Zabrze (Poland) <sup>54</sup>       | 45.58  | 7.03   | 6.33 | 0.82  | 32.23  | 13.04  |       |       | 17210  | 14.48  |       |       |       |       |       | 242.92 |
| Nuevo Leon (Mexico) <sup>55</sup>   | 84.73  | 5.59   | 1.83 | 0.37  | 25.83  | 644.51 |       |       | 88.93  | 33.03  |       |       |       |       |       | 1436.4 |

<sup>a</sup> Present study.

is less than  $1 \times 10^{-6}$ , the local population is regarded as safe; significant when the risk is up to  $1 \times 10^{-4}$  and intolerable when the CR value is  $>1 \times 10^{-4}$ . The findings of this research reveal that CR values for Pb are within the safe limits shown in Fig. 4c, demonstrating that there is no longer a cancer risk from Pb exposure. In contrast, Cr, Co, and Cd show a significant cancer risk, while Ni has exceptionally high CR values (Fig. 4c), indicating a severe cancer threat to the local population. Consequently, the urban air in Islamabad posed a high risk of cancer. Overall, exposure to these toxic metals demonstrates the possibility that an individual would get cancer due to lifetime exposure to these potentially toxic metals. The findings of this research were consistent with those of Joshirvani *et al.*<sup>46</sup> The current investigation has demonstrated a significant carcinogenic risk caused by inhaling airborne particles that contain toxic elements. Therefore, it is necessary to regulate or decrease the causes of emissions of these harmful elements into the atmosphere.

### 3.7 Comparison with reported levels

The current levels of TSP and selected trace metals are compared with those published internationally, as shown in Table 4. It was noted that the mean level of TSP in the atmosphere of Islamabad is significantly lower than those in some Asian cities, including Lahore,<sup>47</sup> Zabol,<sup>14</sup> Delhi,<sup>48</sup> Huainan,<sup>43</sup> and Kathmandu.<sup>49</sup> Several Asian cities, including Seoul,<sup>40</sup> Pohang,<sup>50</sup> and Hat Yai,<sup>51</sup> have low concentrations of TSP compared to current levels. However, current levels of TSP are comparable to those in Beijing,<sup>21</sup> Maros Regency,<sup>52</sup> and Jeddah.<sup>53</sup> Furthermore, the current TSP concentration is significantly higher than in Zabrze, Poland, and Nuevo Leon, Mexico.<sup>54,55</sup>

A comparison of metal concentrations (Table 4) revealed that the current levels of almost all metals were significantly lower than those reported in severely polluted urban cities in Asia, including Lahore, Pakistan,<sup>47</sup> Delhi, India,<sup>48</sup> Huainan and Qingdao, China,<sup>15,43</sup> Zabol, Iran,<sup>14</sup> Maros Regency, Indonesia,<sup>52</sup> and Jeddah, Saudi Arabia.<sup>53</sup> The atmospheric concentration of Cr in this investigation was much lower than that in severely contaminated cities in Asia, including Maros, Lahore, Qingdao, and Delhi, as shown in Table 4. Similarly, the current level of Pb in airborne particulates was also lower than those reported for Maros, Lahore, Zabol, Dhaka, and Qingdao. In contrast, it is very high compared to Seoul (South Korea), Yenagoa (Nigeria), and Leon (Mexico). The average Mn level was comparable to Leon's.<sup>55</sup> Similarly, the mean level of Cd in the atmosphere of Islamabad was also comparable to those found in Beijing, China.<sup>21</sup> Moreover, when metal levels were compared with the European city of Zabrze, it was found that all metal levels (Cr, Ni, Cd, Pb, and Cu) in Zabrze (Poland) were low except for Zn, which had a significantly high concentration.<sup>54</sup> The comparison shows that current particulate matter (PM) and trace metal levels are considerably higher than those reported in Asian, European and American urban areas because they have more stringent environmental regulations.<sup>56-60</sup> However, these were comparable with some urban areas globally and significantly

lower than those in overpopulated cities, especially in South Asia.

## 4. Conclusions

This study revealed considerable variations in the levels of total suspended particles and trace metals in the atmosphere of Islamabad. The TSP levels were found to be higher than the permissible limits specified by the World Health Organisation (WHO) and the United States Environmental Protection Agency (USEPA). The study indicated that the concentration of Ni exceeded WHO guidelines, which can be a cause of major concern. Most metals in atmospheric particulates were observed to be random. The results of the correlation analysis indicated several strong mutual associations between the total suspended particulate matter and trace metals, thus suggesting their common sources. Multivariate analyses (PCA and CA) were conducted to identify the main sources of pollution. It was found that automobile/industrial emissions, fuel combustion, and wind-blown re-suspended dust were the major sources of pollution. The enrichment factor and the geoaccumulation index revealed that the urban atmosphere was heavily contaminated with Ag, Cd, Ni, and Pb, indicating the impact of human activities on the environment. Furthermore, Ni was found to exhibit the highest ecological risk among the metals. The calculated hazard quotient values for Ni and Co exceeded the safe limit ( $HQ > 1$ ), thereby indicating a significant non-carcinogenic threat to human health. Additionally, the study revealed that Ni posed the highest carcinogenic risk, while Pb showed the lowest risk. Moreover, a comparison of the current TSP and metal levels showed that they were considerably higher than the levels reported in urban areas of Europe and North America. Nevertheless, these levels were comparable to those found in some urban areas worldwide and significantly lower than those observed in overpopulated cities, particularly in South Asia. The study thus highlights the urgent need to control these toxic pollution sources, particularly Ni, Cd, Pb and Ag, in the local atmosphere of Islamabad. Overall, the findings of this study provide an essential source of information for regulating air quality and ensuring public health. The current investigation emphasised the need for measures to mitigate air pollution in Islamabad, Pakistan.

## Author contributions

Rashida Nazir: methodology, investigation, data curation, formal analysis, validation, writing original draft. Riffat Parveen: visualization, resources, formal analysis, reviewing and editing. Munir H. Shah: conceptualization, visualization, resources, supervision, project administration, funding acquisition, writing/reviewing and editing. All authors have read and approved the final manuscript.

## Conflicts of interest

The authors declare that there are no conflicts of interest regarding the publication of this manuscript.



## Data availability

The data supporting this article have been included in the manuscript and as part of the supplementary information (SI). Supplementary information is available. See DOI: <https://doi.org/10.1039/d5ea00131e>.

## Acknowledgements

Funding provided by the Higher Education Commission, Government of Pakistan, to complete this project (NRPU Project No. 6176) is gratefully acknowledged. We are also grateful to Quaid-i-Azam University, Islamabad, for providing the laboratory space for conducting this research.

## References

- 1 A. Talbi, Y. Kerchich, R. Kerbach and M. Boughedaoui, Assessment of annual air pollution levels with PM<sub>1</sub>, PM<sub>2.5</sub>, PM<sub>10</sub> and associated heavy metals in Algiers, Algeria, *Environ. Pollut.*, 2018, **232**, 252–263.
- 2 A. Mallongi, R. D. Astuti, R. Amiruddin, M. Hatta and A. U. Rauf, Identification source and human health risk assessment of potentially toxic metal in soil samples around karst watershed of Pangkajene, Indonesia, *Environ. Nanotechnol., Monit. Manage.*, 2022, **17**, 100634.
- 3 A. Ghadrshenas, T. Tabatabaie, F. Amiri and A. R. Pazira, Spatial distribution, sources identification, and health risk assessment polycyclic aromatic hydrocarbon compounds and polychlorinated biphenyl compounds in total suspended particulates (TSP) in the air of South Pars Industrial region-Iran, *Environ. Geochem. Health*, 2022, **14**, 1–9.
- 4 D. Bousiotis, L. N. Alconcel, D. C. Beddows, R. M. Harrison and F. D. Pope, Monitoring and apportioning sources of indoor air quality using low-cost particulate matter sensors, *Environ. Int.*, 2023, **174**, 107907.
- 5 S. Sobhanardakani, Human health risk assessment of potentially toxic heavy metals in the atmospheric dust of city of Hamedan, west of Iran, *Environ. Sci. Pollut. Res.*, 2018, **25**, 28086–28093.
- 6 S. Sobhanardakani, Ecological and human health risk assessment of heavy metal content of atmospheric dry deposition, a case study: Kermanshah, Iran, *Biol. Trace Elem. Res.*, 2019, **187**, 602–610.
- 7 A. Gladovic, B. Petrovic, D. Vukelic, A. Buha Djordjevic, M. Curcic, D. Dukic-Cosic, A. Sostaris, B. Antonijevic and Z. Bulat, Carcinogenic and human health risk assessment of children's and adults' exposure to toxic metalloids from air PM<sub>10</sub> in critical sites of the Republic of Serbia, *Environ. Sci. Pollut. Res.*, 2023, **30**(22), 61753–61765.
- 8 R. Akoto and A. K. Anning, Heavy metal enrichment and potential ecological risks from different solid mine wastes at a mine site in Ghana, *Environ. Adv.*, 2021, **3**, 100028.
- 9 A. Baidourela, L. Liu, K. Zhayimu, C. Pan, R. Manglike, X. Peng and M. Abudukadeer, Distribution characteristics and correlation of heavy metals in soil and total suspended particles of Urumqi City, *Int. J. Environ. Sci. Technol.*, 2022, **19**, 4947–4958.
- 10 J. Torkashvand, A. J. Jafari, P. K. Hopke, A. Shahsavani, M. Hadei and M. Kermani, Airborne particulate matter in Tehran's ambient air, *J. Environ. Health Sci. Eng.*, 2021, **19**, 1179–1191.
- 11 M. C. Turner, Z. J. Andersen, A. Baccarelli, W. R. Diver, S. M. Gapstur, C. A. Pope III, D. Prada, J. Samet, G. Thurston and A. Cohen, Outdoor air pollution and cancer: An overview of the current evidence and public health recommendations, *Ca-Cancer J. Clin.*, 2020, **70**, 460–479.
- 12 M. Hadei and K. Naddafi, Cardiovascular effects of airborne particulate matter: a review of rodent model studies, *Chemosphere*, 2020, **242**, 125204.
- 13 E. Lavigne, R. Talarico, A. Van Donkelaar, R. V. Martin, D. M. Stieb, E. Crighton, S. Weichenthal, M. Smith-Doiron, R. T. Burnett and H. Chen, Fine particulate matter concentration and composition and the incidence of childhood asthma, *Environ. Int.*, 2021, **152**, 106486.
- 14 R. D. Behrooz, D. G. Kaskaoutis, G. Grivas and N. Mihalopoulos, Human health risk assessment for toxic elements in the extreme ambient dust conditions observed in Sistan, Iran, *Chemosphere*, 2021, **262**, 127835.
- 15 X. Liu, Y. Wang, R. Liu, Y. Zhang, L. Shao, K. Han and Y. Zhang, Pollution characteristics, source identification and potential ecological risk of 50 elements in atmospheric particulate matter during winter in Qingdao, *Arabian J. Geosci.*, 2022, **15**, 233.
- 16 C. L. Kao, G. C. Fang, Y. H. Chen and Y. J. Zhuang, Applying principal component, health risk assessment, source identification for metallic elements of ambient air total suspended particulates at Taiwan Scientific Park, *Environ. Geochem. Health*, 2023, **45**, 809–824.
- 17 Z. Cheng, S. Wang, L. Qiao, H. Wang, M. Zhou, X. Fu, S. Lou, L. Luo, J. Jiang, C. Chen and X. Wang, Insights into extinction evolution during extreme low visibility events: Case study of Shanghai, China, *Sci. Total Environ.*, 2018, **618**, 793–803.
- 18 L. Han, Z. Sun, J. He, Y. Hao, Q. Tang, X. Zhang, C. Zheng and S. Miao, Seasonal variation in health impacts associated with visibility in Beijing, China, *Sci. Total Environ.*, 2020, **730**, 139149.
- 19 M. H. Bashir, H. R. Ahmad, G. Murtaza and M. F. Nawaz, Spatial distribution of heavy metals, source identification, risk assessment, and particulate matter in the M4 motorway, *Environ. Monit. Assess.*, 2023, **195**, 1541.
- 20 U. Panda, R. Boopathy, H. S. Gadhavi, K. Renuka, S. S. Gunthe and T. Das, Metals in coarse ambient aerosol as markers for source apportionment and their health risk assessment over an eastern coastal urban atmosphere in India, *Environ. Monit. Assess.*, 2021, **193**, 311.
- 21 L. Cui, Z. Wu, P. Han, Y. Taira, H. Wang, Q. Meng, Z. Feng, S. Zhai, J. Yu, W. Zhu and Y. Kong, Chemical content and source apportionment of 36 heavy metal analysis and health risk assessment in the aerosol of Beijing, *Environ. Sci. Pollut. Res.*, 2020, **27**, 7005–7014.



- 22 ATSDR, *Annual Report, Protecting People from Harmful Environmental Exposures*, Agency for Toxic Substances and Disease Registry, 2019, [www.atsdr.cdc.gov/2019atsdrannualreport/index.html](http://www.atsdr.cdc.gov/2019atsdrannualreport/index.html).
- 23 F. Ahmed, M. H. Shah and N. Shaheen, Diurnal, and nocturnal variations of trace metals in urban atmospheric particulate matter from Islamabad, Pakistan, *Environ. Earth Sci.*, 2014, **71**, 817–826.
- 24 R. Nazir and M. H. Shah, Study of pollution status and health risks for selected metals in PM<sub>10</sub> from Islamabad, Pakistan, *Int. J. Environ. Sci. Technol.*, 2024, **21**(16), 10059–10074.
- 25 T. Mehmood, I. Ahmad, S. Bibi, B. Mustafa and I. Ali, Insight into monsoon for shaping the air quality of Islamabad, Pakistan, comparing the magnitude of health risk associated with PM<sub>10</sub> and PM<sub>2.5</sub> exposures, *J. Air Waste Manage. Assoc.*, 2020, **70**, 1340–1355.
- 26 I. Shahid, M. Kistler, M. Z. Shahid and H. Puxbaum, Aerosol chemical characterization and contribution of biomass burning to particulate matter at a residential site in Islamabad, Pakistan, *Aerosol Air Qual. Res.*, 2019, **19**, 148–162.
- 27 D. Lv, Y. Chen, T. Zhu, T. Li, F. Shen, X. Li and T. Mehmood, The pollution characteristics of PM<sub>10</sub> and PM<sub>2.5</sub> during summer and winter in Beijing, Suning, and Islamabad, *Atmos. Pollut. Res.*, 2019, **10**, 1159–1164.
- 28 I. M. Sheikh, M. K. Pasha, V. S. Williams, S. Q. Raza and K. S. A. Khan, in, *Environmental Geology of the Islamabad-Rawalpindi Area, Northern Pakistan*, *Regional Studies of the Potwar Plateau Area, Northern Pakistan*, ed. P. D. Warwick and B. R. Wardlaw, US Geological Survey Bulletin, 2007, 2078, pp. 1–9.
- 29 US-Environmental Protection Agency, Method IO-2.1: Sampling of Ambient Air for Total Suspended Particulate Matter (SPM) and PM<sub>10</sub> using High Volume Sampler, EPA/625/R-96/010a, in *Compendium of Methods for the Determination of Inorganic Compounds in Ambient Air*, Cincinnati, USA, 1999.
- 30 Comité Européen de Normalisation (CEN), Standard Gravimetric Measurement Method for the Determination of the PM<sub>2.5</sub> Mass Fraction of Suspended Particulate Matter, EN 14907:2005, *Ambient Air Quality*, European Committee for Standardization, Brussels, Belgium, 2005.
- 31 US-Environmental Protection Agency, Method IO-3.1: Selection, Preparation and Extraction of Filter Material, EPA/625/R-96/010a, in *Compendium of Methods for the Determination of Inorganic Compounds in Ambient Air*, Cincinnati, OH, 1999.
- 32 US-Environmental Protection Agency, Method IO-3.2: Determination of Metals in Ambient Particulate Matter Using Atomic Absorption (AA) Spectroscopy, EPA/625/R-96/010a, in *Compendium of Methods for the Determination of Inorganic Compounds in Ambient Air*, Cincinnati, OH, 1999.
- 33 S. R. Taylor and S. M. McLennan, *The Continental Crust: its Composition and Evolution*, Blackwell Sci. Publ., 1985, Oxford, p. 330.
- 34 M. Zhi, X. Zhang, K. Zhang, S. J. Ussher, W. Lv, J. Li, J. Gao, Y. Luo and F. Meng, The characteristics of atmospheric particles and metal elements during winter in Beijing: Size distribution, source analysis, and environmental risk assessment, *Ecotoxicol. Environ. Saf.*, 2021, **1211**, 111937.
- 35 K. Ulutas, Spatial distribution, contamination levels, source identification and human health risk assessment of potentially toxic elements in street dust in the urban area in Libya, *Soil Sediment Contam.*, 2023, **32**, 125–146.
- 36 L. Håkanson, An ecological risk index for aquatic pollution control—a sedimentological approach, *Water Res.*, 1980, **14**(8), 975–1001.
- 37 USEPA, Regional Screening Levels (RSLs) – Generic Tables, 2016, <https://www.epa.gov/risk/regional-screening-levels-rsls-generic-tables-may-2016>.
- 38 World Health Organization, New WHO Global Air Quality Guidelines Aim to Save Millions of Lives from Air Pollution, 2021, <https://www.int/news/item/>.
- 39 M. Abdulaziz, A. Alshehri, H. Badri, A. Summan and A. Sayqal, Concentration level and health risk assessment of heavy metals in PM<sub>2.5</sub> in ambient air of Makkah City, Saudi Arabia, *Pol. J. Environ. Stud.*, 2022, **5**, 31.
- 40 E. Choi, S. M. Yi, Y. S. Lee, H. Jo, S. O. Baek and J. B. Heo, Sources of airborne particulate matter-bound metals and spatial-seasonal variability of health risk potentials in four large cities, South Korea, *Environ. Sci. Pollut. Res.*, 2022, **29**, 28359–283574.
- 41 G. Zhang, C. Ding, X. Jiang, G. Pan, X. Wei and Y. Sun, Chemical compositions and sources contribution of atmospheric particles at a typical steel industrial urban site, *Sci. Rep.*, 2020, **10**, 7654.
- 42 P. S. Oetari, S. P. Hadi and H. S. Huboyo, Trace elements in fine and coarse particles emitted from coal-fired power plants with different air pollution control systems, *J. Environ. Manage.*, 2019, **250**, 109497.
- 43 J. Ou, L. Zheng, Q. Tang, M. Liu and S. Zhang, Source analysis of heavy metals in atmospheric particulate matter in a mining city, *Environ. Geochem. Health*, 2022, **44**, 979–991.
- 44 F. Khanum, M. N. Chaudhry, G. Skouteris, D. Saroj and P. Kumar, Chemical composition and source characterization of PM<sub>10</sub> in urban areas of Lahore, Pakistan, *Indoor Built Environ.*, 2021, **30**, 924–937.
- 45 N. Gujre, S. Mitra, A. Soni, R. Agnihotri, L. Rangan, E. R. Rene and M. P. Sharma, Speciation, contamination, ecological and human health risks assessment of heavy metals in soils dumped with municipal solid wastes, *Chemosphere*, 2021, **262**, 128013.
- 46 A. Joshirvani, M. R. Samarghandi and M. Leili, PM<sub>10</sub> concentration, its potentially toxic metals content, and human health risk assessment in Hamadan, Iran, *Clean: Soil, Air, Water*, 2021, **49**, 2000174.
- 47 M. I. Jalees and Z. Asim, Statistical modelling of atmospheric trace metals in Lahore, Pakistan for correlation and source identification, *Environ. Earth Sci.*, 2016, **75**, 842.
- 48 R. Jangirh, S. Ahlawat, R. Arya, A. Mondal, L. Yadav, G. Kotnala, P. Yadav, N. Choudhary, M. Rani, R. Banoo and A. Rai, Gridded distribution of total suspended particulate matter (TSP) and their chemical



- characterization over Delhi during winter, *Environ. Sci. Pollut. Res.*, 2022, **29**, 17892–17918.
- 49 L. Maharjan, L. Tripathee, S. Kang, B. Ambade, P. Chen, H. Zheng, Q. Li, K. L. Shrestha and C. M. Sharma, Characteristics of atmospheric particle-bound polycyclic aromatic compounds over the Himalayan Middle Hills: implications for sources and health risk assessment, *Asian J. Atmos. Environ.*, 2021, **15**, 1–19.
- 50 K. M. Baek, M. J. Kim, J. Y. Kim, Y. K. Seo and S. O. Baek, Characterization and health impact assessment of hazardous air pollutants in residential areas near a large iron-steel industrial complex in Korea, *Atmos. Pollut. Res.*, 2020, **11**, 1754–1766.
- 51 M. Inerb, W. Phairuang, P. Paluang, M. Hata, M. Furuuchi and P. Wangpakapattanawong, Carbon, and trace element compositions of total suspended particles (TSP) and nanoparticles (PM<sub>0.1</sub>) in ambient air of southern Thailand and characterization of their sources, *Atmosphere*, 2022, **13**, 626.
- 52 A. U. Rauf, A. Mallongi, K. Lee, A. Daud, M. Hatta, W. Al Madhoun and R. D. Astuti, Potentially toxic element levels in atmospheric particulates and health risk estimation around industrial areas of Maros, Indonesia, *Toxics*, 2021, **12**, 328.
- 53 M. Cusack, J. M. Arrieta and C. M. Duarte, Source Apportionment and elemental composition of atmospheric total suspended particulates (TSP) over the red seacoast of Saudi Arabia, *Earth Syst. Environ.*, 2020, **4**, 777–788.
- 54 M. Rachwal, M. Wawer, M. Jablonska, W. Rogula-Kozłowska and P. Rogula-Kopiec, Geochemical and mineralogical characteristics of the airborne particulate matter about the human health risk, *Minerals*, 2020, **10**, 866.
- 55 L. T. Gonzalez, F. L. Rodriguez, M. Sanchez-Dominguez, A. Cavazos, C. Leyva-Porras, L. G. Silva-Vidaurre, K. A. Askar, B. I. Kharissov, J. V. Chiu and J. A. Barbosa, Determination of trace metals in TSP and PM<sub>2.5</sub> materials collected in the Metropolitan Area of Monterrey, Mexico: A characterization study by XPS, ICP-AES and SEM-EDS, *Atmos. Res.*, 2017, **196**, 8–22.
- 56 S. A. Shammi, A. Salam and M. A. H. Khan, Assessment of heavy metal pollution in the agricultural soils, plants, and in the atmospheric particulate matter of a suburban industrial region in Dhaka, Bangladesh, *Environ. Monit. Assess.*, 2021, **193**, 104.
- 57 S. R. Karimi, N. Mansouri, L. Taghavi and M. Moeinaddini, Receptor modelling and health risk assessment of suspended heavy metal particles in Tehran's District 21, *Int. J. Environ. Sci. Technol.*, 2023, **20**, 931–942.
- 58 M. Ahmed, X. Guo and X. M. Zhao, Determination and analysis of trace metals and surfactant in air particulate matter during biomass burning haze episode in Malaysia, *Atmos. Environ.*, 2016, **141**, 219–229.
- 59 S. A. Uzoekwe and E. D. Ajayi, Trace metals concentration assessment in urban particulate matter in Yenagoa and its environs, *J. Appl. Sci. Environ. Manage.*, 2018, **22**, 134–140.
- 60 Q. Wang, S. Lu, Y. Lin, C. E. Enyoh, T. Chowdhury, M. H. Rabin, M. R. Islam, Y. Guo and W. Wang, Pollution levels and health risk assessment of potentially toxic metals of size-segregated particulate matter in rural residential areas of high lung cancer incidence in Fuyuan, China, *Environ. Geochem. Health*, 2023, **45**(6), 2869–2889.

